Solid State Phenomena *Online: 2009-10-28*
ISSN: 1662-9779, Vols. 156-158, pp 1-10
doi:10.4028/www.scientific.net/SSP.156-158.1

Influence of Defects on Solar Cell Characteristics

Otwin Breitenstein[1,a], Jan Bauer[1,b], Pietro P. Altermatt[2,3,c], and Klaus Ramspeck[3,d]

[1]Max Planck Institute of Microstructure Physics, Weingerg 2, 06120 Halle, Germany

[2]Leibniz University Hannover, Dep. Solar Energy, Appelstr. 2, 30167 Hannover, Germany

[3]ISFH Hameln/Emmerthal, Am Ohrberg 1, 31860 Emmerthal, Germany

[a]breiten@mpi-halle.mpg.de, [b]jbauer@mpi-halle.mpg.de, [c]altermatt@solar.uni-hannover.de, [d]ramspeck@isfh.de

Keywords: Solar cells, I-V characteristic, ohmic shunts, ideality factor, recombination current, leakage current, breakdown, avalanche

Abstract. The current-voltage (I-V) characteristics of most industrial silicon solar cells deviate rather strongly from the exponential behavior expected from textbook knowledge. Thus, the recombination current may be orders of magnitude larger than expected for the given material quality and often shows an ideality factor larger than 2 in a wide bias-range, which cannot be explained by classical theory either. Sometimes, the cells contain ohmic shunts although the cell's edges have been perfectly insolated. Even in the absence of such shunts, the characteristics are linear or super-linear under reverse bias, while a saturation would be classically expected. Especially in multicrystalline cells the breakdown does not tend to occur at -50 V reverse bias, as expected, but already at about -15 V or even below. These deviations are typically caused by extended defects in the cells. This paper reviews the present knowledge of the origin of such non-ideal I-V characteristics of silicon solar cells and introduces new results on recombination involving coupled defect levels.

Introduction

The classical theory of p-n junction diodes was established by Shockley [1] and was later extended by recombination in the p-n junction depletion region by Sah, Noyce, and Shockley [2]. According to this theory, the dark current-voltage (I-V) characteristics are described by the so-called "two diode model":

$$I = I_{01}\left(\exp\frac{eV}{kT}-1\right)+I_{02}\left(\exp\frac{eV}{nkT}-1\right) \qquad (1)$$

Here I_{01} and I_{02} are the saturation currents, and *n* is the so-called ideality factor. In order to be independent of the cell area *A*, the current-densities J are given instead of the currents I in (1). According to [2] and also to recent, more realistic numerical simulations [3], J_{02} should be in the order of 10^{-10} A/cm^2 for relatively poor material with a excess carrier lifetime of τ = 10 µs, and the ideality factor should be maximally n = 2. Also modern textbooks such as Sah [4] describe the current-voltage (I-V) characteristic of solar cells on these theoretical grounds, which predicts that the reverse current-density saturates for a reverse bias below -100 mV to a constant value of $-(J_{01} + J_{02})$. Advanced theory predicts avalanche breakdown above a certain reverse bias, which is below -50 V for typical solar cells having a base doping concentration of 10^{16} cm^{-3} [4]. Some authors use only the second term in (1), i.e. a one-diode model, for the approximation of the I-V characteristics [5]. Such an approximation may be appropriate in a limited bias range around the maximum power point (mpp), where the dark characteristics most strongly influence the efficiency. Note that the two-diode model (1) does not contain any ohmic shunt resistance R_p of currents that

circumvent the p-n junction, nor a series resistance R_s. It is common practice to include also these entities in a one- or two-diode model via an equivalent circuit [5]:

$$I = I_{01}\left(\exp\frac{e(V - IR_s)}{kT} - 1\right) + I_{02}\left(\exp\frac{e(V - IR_s}{nkT} - 1\right) + \frac{V - IR_s}{R_{sh}} \quad . \qquad (2)$$

However, when doing so, nothing about the nature especially of R_p can be said.

High-efficiency solar cells, which are fabricated from monocrystalline material by using planar technology, may follow the predictions of the 2-diode model (2) rather precisely. However, industrially fabricated solar cells, especially those made from multicrystalline (MC) material, usually behave very differently at a forward bias below 0.6 V. We call these deviations "non-ideal" diode behavior. There are different aspects of this non-ideal behavior. In the absence of ohmic shunts, the external current in the dark is equal to the recombination rate in the device, i.e. it is solely produced by recombination. The current-contribution behaving most ideally is caused by SRH recombination in the quasi-neutral regions. This current-contribution is traditionally called the "diffusion current", and because it has an ideality factor = 1, it is described by the first term in (1). According to [1], J_{01} is proportional to $1/\sqrt{\tau}$. Indeed, the magnitude of J_{01} is usually as expected from classical theory [1] even in industrial MC cells, provided that the lifetime τ is correctly averaged across the cell's area: Regions with a high J_{01} (low τ) are connected in parallel to regions of low J_{01} (high τ), and $1/\sqrt{\tau}$ has to be averaged (instead of averaging τ arithmetically) [6]. It will be shown below that the characteristics of real solar cells behave very differently to the predictions of [2] because recombination in the depletion region contributes significantly to the cell's total external current. This type of current-contribution is traditionally called the "recombination current", although any current-contribution in the dark is caused by recombination. Also, the breakdown behavior of real (especially of MC) solar cells under reverse bias deviates significantly from the predictions in [4]. Finally, in many cases an ohmic parallel resistance R_p can be observed in real solar cells, which also cannot be described by any classical diode model. So the three general aspects of non-ideal diode behavior are (1) the amount of recombination as a function of bias, (2) the breakdown behavior, and (3) the nature of ohmic shunts. These aspects will be discussed separately in the following.

Experimental

The first evidence about the origin of non-ideal current contributions came from I-V characteristics measured on cells of different size [7]. By successively cutting a solar cell into smaller pieces, it was observed that the area-related density of the recombination current, which showed an ideality factor larger than 2, increases with smaller sample size. This lead to the conclusion that the recombination current flows essentially at the edge of the cell, which was confirmed later by many other authors, e.g. [3, 8]. The increasing application of lock-in thermography (LIT) techniques to solar cell characterization [9-11] was the key for a detailed investigation of the origins of non-ideal diode behavior. LIT means that heat generation in a device is periodically pulsed while the device is imaged with an infrared camera, and the images are processed in a way to detect only the periodic temperature modulation. By averaging over a certain acquisition time, temperature modulations below 100 μK can be detected after 1/2 hour [10]. Moreover, due to the dynamic character of this technique, lateral heat diffusion is suppressed, so that LIT images provide a much better spatial resolution than steady-state thermograms do. The basic variant of this technique is detection without light irradiation and is called Dark Lock-In Thermography (DLIT) [11]. Because the signal is in this case a quantitative measure of the locally flowing current density, DLIT literally allows us to "see where the current in a device flows". Since not only the dark current flowing in a solar cell but also all other elementary processes in an illuminated cell are leading to the local generation or

consumption of heat (including Peltier effects), LIT has become a very successful technique for investigating local physical processes in solar cells [11, 12].

Recombination current

Experimental findings. Fig. 1 shows a measured I-V characteristics in forward-bias of a typical 156x156 mm^2 sized MC solar cell. This cell has no ohmic shunts. The best fit with equation (1) below a bias of 0.3 V yields $J_{02} = 3.3\times10^{-7}$ A/cm^2 and n = 3. This large ideality factor cannot be explained with classical diode theory, and also the J_{02} is about 3 orders of magnitude larger than expected by [2]. Fig. 2 shows a typical DLIT image of a cell like the one measured in Fig. 1, except that it shows some weak ohmic shunts. An image was taken at a forward bias of 0.5 V, which is close to the maximum power point (mpp) under illumination, and an other image at a reverse bias of -0.5 V. Under reverse bias, the exponential current contributions are negligibly small, hence only currents along some ohmic shunts paths are visible. At +0.5 V, both the diffusion and the recombination currents flow in considerable amounts. Most of the structures visible in forward bias but invisible in reverse bias are caused by local recombination currents at the edge region and in a number of spots in the interior area. The bright line at the bottom left is due to a weak scratch. In reverse bias, only one spot at the bottom right and some regions at the edge show some ohmic conductivity. The weak cloud-like structures in the area of (a) are local maxima of the diffusion currents in low lifetime regions. Thermal ideality factor imaging ([10], not shown here) has revealed an ideality factor of n = 1 in these regions (proving that this is a diffusion current), but ideality factors of n = 3 and above in the regions of recombination current. All local features except the cloud-like ones in (a), which do not appear in (b), are called "non-linear shunts", which are basically due to locally extended defects leading to a local recombination current. Intentionally made scratches on solar cells behave like typical non-linear shunts. By comparing the I-V characteristics of scratches made with different loads it had been found that the ideality factor increases with increasing load, hence with increasing local concentration of defect states [13].

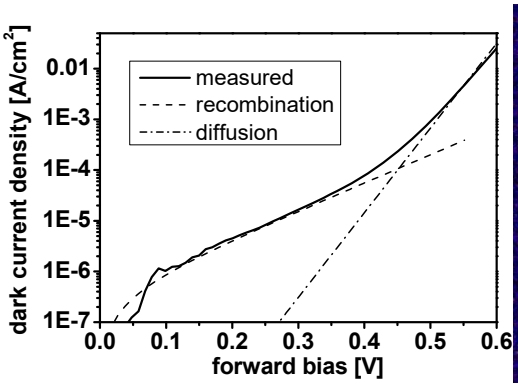

Fig. 1: Dark I-V characteristic of a typical industrial multicrystalline silicon solar cell

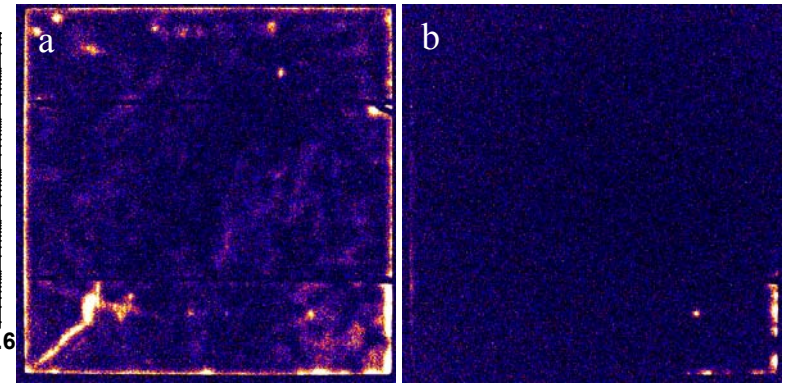

Fig. 2: DLIT images of a typical industrial multicrystalline silicon solar cell, (a) under +0.5 V forward bias, (b) under -0.5 V reverse bias

Previous explanations. Already Queisser [14] has investigated the unexpectedly large ideality factor of solar cells and has suspected its cause in metallic precipitates in the material. However, such precipitates are not present in typical solar cells. Kaminski et al. [15] have attributed this current to trap-assisted tunnelling or field-assisted recombination at point defect levels. Since for increasing forward bias the electric field in the depletion region reduces, trap-assisted tunnelling becomes less probable for increasing forward bias, which is equivalent to a saturation effect leading to an increase of the ideality factor. However, the concentration of point defects in solar cells is usually much too small to account for the measured magnitude of the recombination current. Schenk and Krumbein [16] have tried to solve this problem by assuming two-level (pair)

recombination with participation of at least one shallow level. Because shallow levels have a spatially more extended wave function, trap-assisted tunnelling is much more probable for shallow levels than for deep levels. However, since single shallow levels show a very weak coupling to the more distant band, Schenk and Krumbein had to assume infinitely strong coupling between the shallow level and a second deep level or a complimentary shallow level. In reality, this coupling should be exponentially dependent on the distance of the levels to each other, so assuming infinitely strong coupling is a rather strong assumption. Nevertheless, also Schenk was unable to explain the magnitude of measured recombination currents based on the concentration of known point defect levels. Breitenstein and Heydenreich [7] and later also other authors [3, 8] have published measurements of recombination currents that are not proportional to the area but to the circumference-length of a cell. Hence, they are supposedly caused by recombination at surface states where the p-n junction reaches the surface. This edge recombination current-density must be given in units of A/cm, i.e. per cm edge line, instead of A/cm^2 as was previously done. Kühn et al. [17] found by means of device simulations that, if the edge region is assumed to be a surface without surface charge, the finite thermal velocity of carriers limits the SRH recombination current-density at the surface to values below 10^{-8} A/cm, which is much lower than typically measured values. These authors showed that this limitation may be overcome by regarding depletion or inversion of the surface, whereby the region of recombination extends into the cell's interior. McIntosh [3] has simulated the edge current by assuming SRH recombination, leading to an ideality factor of maximally 2. However, he took the series resistance in the emitter layer on the way to the edge region into account. This resistance indeed tends to increase the ideality factor. However, it creates only a "hump" in the I-V-characteristic, rather than a large ideality factor over an extended bias range. This theory cannot explain large ideality factors at low forward biases below 0.2 V, since at such low voltages the recombination current is so small that the series resistance has a negligible effect. It was shown in [13] that indeed the series resistance increases the ideality factor of the recombination current, but it is not the primary reason for a large ideality factor. There must be other reasons leading to a large ideality factor for recombination at extended defects like surfaces.

Coupled defect level (CDL) recombination. Schenk and Krumbein [16] already considered recombination via two coupled levels as a cause for the observed recombination current. However, they investigated cells made of epitaxially grown materials and therefore assumed that such currents are caused by a homogeneous distribution of point defects. To achieve the measured magnitudes of current-densities, they require an unrealistic high density of defect levels. This is so because recombination via coupled defects requires an overlap of the wave functions of the participating levels. Since the spatial extension of the wave function of deep levels is very small (typically some nm), Schenk and Krumbein assumed that at least one shallow level participates, whose wave function is considerably more extended. Moreover, they assumed infinitely strong coupling between the two levels, which can only be assumed for levels that are situated very closely together. The increased ideality factor was basically due to the field dependence of the carrier capturing probability by the shallow level, similar as in the model of Kaminski [15].

However, if we assume that the recombination current flows locally in the locations of extended defects like scratches or surfaces, very high local concentrations of defect levels can be realistically assumed. While oxidized surfaces may show already a density of defect states of about 10^{12} cm^{-2} – corresponding to a mean distance between the defects of 10 nm – a highly disturbed surface like a scratch, a laser cut, or an interface to a precipitate, may easily have a thousandfold higher defect density – corresponding to a mean distance well below 1 nm, which makes deep defect interaction probable. In this case, the levels may be situated so close to each other that it is not necessary anymore to assume one level to be shallow. In [13], we have qualitatively compared the above-mentioned model of Schenk and Krumbein with a simple deep donor-acceptor pair recombination model assuming constant capture coefficients and taking the level coupling as a (distance-dependent) parameter. It was found that also this sort of pair recombination model explains

sufficiently large ideality factors due to a saturation of the inter-level recombination: the total recombination rate then increases with increasing minority carrier density slower than in case of single level recombination. The treatment in [13] was only qualitative. In the following, we present new device simulations of recombination via coupled donor-acceptor levels that are both situated deep in the bandgap, performed with the numerical device simulator Sentaurus [18].

In the following simulations, we incorporate a 10 μm wide, heavily defected region into the p-n junction of a PERL cell where CDL recombination locally predominates. To explore the effects on the ideality factor n, we vary the coupling rate between the two defects, r_{12}, the energy levels E_1 and E_2 of the first and second defect, and also the lifetime parameters of the first defect (τ_{n1}) and the second defect (τ_{p2}) symmetrically, i.e. $\tau_{n1} = \tau_{p2}$. In constast, $\tau_{p1} = \tau_{n1} = 0$ is chosen to obtain ideal donor- and acceptor-like behavior.

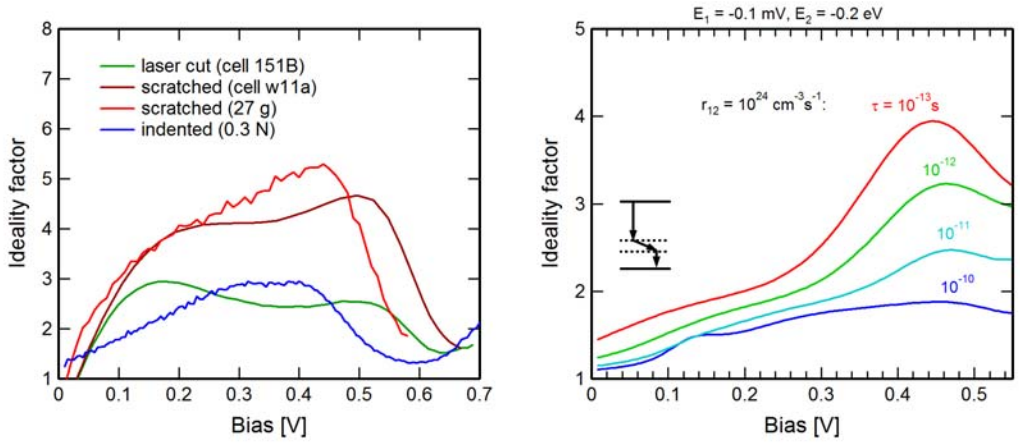

Fig. 3. Left: experimentally determined ideality factors of the dark characteristics of cells that were laser cut, scratched or indented. Right: simulated ideality factors of a PERL cell in the dark, containing a heavily defected region where recombination via two coupled neighboring defects dominates. The second defect level is situated lower in the gap than the first one.

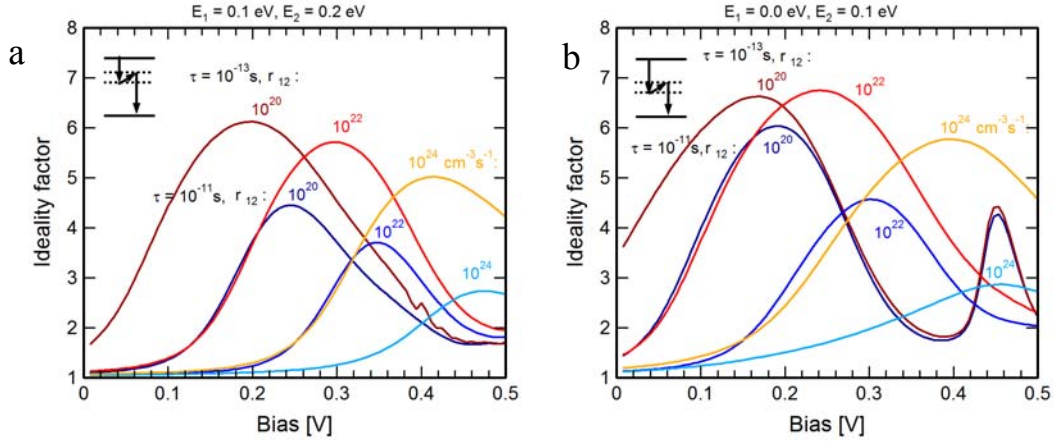

Fig. 4. Simulated ideality factor of a PERL cell in the dark, containing a heavily defected region where recombination via two coupled neighboring defects dominates. The electron is thermally excited into a neighboring defect level that is situated higher in the energy gap. Varied are the lifetime parameters τ and the coupling rate between the neighbors, r_{12}.

An example is given in Figure 3 (right) for the case that the second defect has lower energy than the first one. Note that the ideality factors tend to peak between 0.3 and 0.5 V forward bias, regardless of the magnitude of τ, r_{12}, or the energy levels (not all variations are shown in Fig. 3). A richer variety of effects can be produced if the second defect is approximately 0.1 eV higher than the first defect, as shown in Fig. 4. The electron, captured by the first defect state, is thermally excited into the second defect state before it recombines. Note that, if the second defect has a higher

energy, the bias where n peaks is sensitive to r_{12}: closer neighbors with higher r_{12} shift the peak of n towards higher forward biases. In addition, the magnitude of n increases with shorter τ. The bias where n peaks is rather insensitive to the magnitude of τ or the energy levels (not all variations are shown in Fig. 4).

The finding that only some parameters affect the ideality factor substantially is important, because in heavily disturbed device regions there are always a variety of defects present (with various τ values and energy levels), whose nearest neighbors have a variety of distances (variety of r_{12} values). Hence, the experimental I-V curve results from a sum over many types of defect pairs. Comparing the four experimental curves of Fig. 3 (left) with the simulated examples, it becomes apparent that these experimental curves can be indeed reconstructed by summing the simulations over a spatial and energetic distribution of defect pairs.

It is not surprising that the behavior of the ideality factor varies from experiment to experiment to some extent, because the distribution of defect pairs does so. There is also some degree of randomness inherent in heavily disturbed regions. Nevertheless, all four experiments show a peak in n between 0.4 and 0.5 V. Our simulations indicate that the peak is caused by defect pairs where the second defect level has lower energy than the first level, as indicated in Figure 3 (right). All four experiments also show a very slow change in n over an extended bias range, typically below 0.5 V. Figure 4 shows that this behavior is possibly caused by a broad distribution of mutual distances between the coupled defects (leading to a distribution of r_{12}) where the second levels has a higher energy than the first level.

The central conclusion from this consideration is that we can explain these two commonly found features of the ideality factor without restriction to a particular defect distribution. Most non-specific, smooth distributions of τ values, energy levels, and r_{12} values will yield these two common features (not shown in this paper). The chosen distribution merely determines the fine-tuning of the ideality factor. If, in contrast, we had to rely on a very specific, improbable distribution in our model to explain experimental ideality factors, our model would have been equally improbable.

Reverse characteristics

Even in the absence of significant ohmic shunts, the reverse characteristics of industrial solar cells are always linear (ohmic) and, starting already at a few Volts reverse bias, are becoming superlinear (breakdown behavior). By performing scratches of different load in previously ideally behaving solar cells, it has been found that the ohmic reverse conductivity, just as the recombination current, drastically increases with increasing load of the scratches [13]. This proves that the ohmic reverse characteristic and the recombination current have one and the same physical origin: They are both due to extended defects with a high density of states crossing the p-n junction. The reverse current of the scratches increased with $\exp(-1/T^{1/4})$, which is the characteristic temperature dependence for variable range hopping conduction according to Mott's theory [19]. Therefore it has been concluded that the ohmic reverse conductivity of industrial solar cells without significant ohmic shunts is due to hopping conduction via states of extended defects e.g. in the edge region or in other regions of non-linear (recombination-induced) shunts [13].

According to established theory, solar cells with a base doping concentration of 10^{16} cm^{-3} should break down by avalanche at a reverse bias above -50 V [4]. In reality, the characteristics may become superlinear already at -5 V, and at about -13 V hard breakdown begins [20]. This breakdown occurs for alcaline textured cells at a somewhat higher voltage than for acidic texture, which is probably a result of the higher roughness of the acidic texture [21]. If a cell in a module is shaded, it may become reverse-biased by the other cells in this string. If breakdown occurs, hot spots may appear which may damage the module. Therefore the physical origin of breakdown sites must be investigated, which can be done e.g. by DLIT. By performing DLIT under various reverse biases and special LIT techniques for imaging the local temperature coefficient, slope, and avalanche multiplication factor [22], the following observations about breakdown in acidically etched industrial MC solar cells were made: Breakdown occurs only locally at certain breakdown

sites, hence there is no areal breakdown below -50 V; all breakdowns occurring are defect-induced. There are several different breakdown mechanisms acting in different bias ranges. Fig. 5 (a) is a forward bias EL image showing grown-in recombination-active crystal defects of the MC material. As the DLIT image (b) shows, at -5 V the reverse current flows mostly in the edge region (hopping conduction?) and in some places in the area, e.g. site "I". At -12 V (c) and above many new breakdown sites appear. They are mostly in positions of recombination-active crystal defects visible in (a), see e.g. site "II". At a reverse bias of -15 V (d) new breakdown sites appear in regions where no significant recombination-active defects were visible in (a), e.g. site "III". Note the different scaling limits of (b), (c), and (d). Thermal measurements of the temperature coefficient (TC) and the slope of such sites have shown that the edge leakage shows a positive TC and a low slope, sites "I" and "II" show a clearly negative TC, and type "II" shows an only slightly negative ore close to zero TC and a medium slope [22]. It has also been found that only breakdown sites of type "III" show significant avalanche multiplication of photo-generated carriers and a high slope [22].

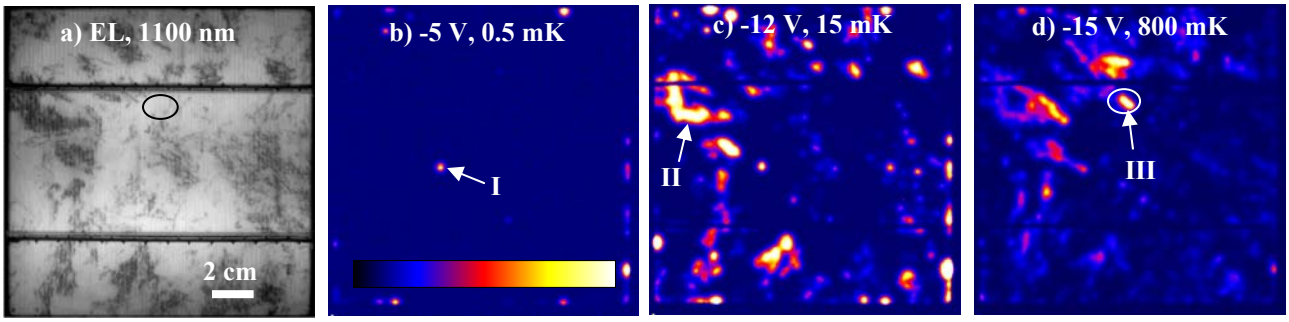

Fig. 5: EL image (a) and DLIT images of a MC cell measured at -5 V (b, scaled to 0.5 mK), -12 V (c, scaled to 15 mK), and -15 V (d, scaled to 800 mK)

As discussed above, the edge leakage sites, which show a linear or only slightly superlinear characteristic and a positive TC, may be due to hopping conduction across surface states crossing the p-n junction in the edge region. The physical reason for the early prebreakdown sites of type "I" is not revealed yet. However, due to their strongly negative TC and low slope, they do not seem to be dangerous for the module. The sites of type "II" are clearly defect-induced and have shown a correlation between their recombination and breakdown activity. Therefore we believe that their breakdown mechanism includes gap states of the defects. The exact mechanism is unclear yet. It is expected to become dominating if upgraded metallurgical grade (UMG) material is used for solar cells. The mechanism of breakdown "III" has been identified as avalanche breakdown at the tips of dislocation-induced etch pits [20]. There, due to field enhancement by the tip effect, the avalanche breakdown voltage reduces locally from -50 V to -13 V [23]. Since this mechanism shows the highest slope of all mechanisms, it dominates at high reverse bias, if etch pits are present.

Ohmic shunts

Ohmic shunts are easily detectable in DLIT by comparing the +0.5 V image with the -0.5 V one, see Figs. 2 (a) and (b). The different types of ohmic shunts appearing in silicon solar cells have been discussed already in [24]. Here we will just present a brief summary. The most trivial type of ohmic shunts is an incompletely opened edge of a cell. Another common type is a crack in the base material, which was present already before cell processing. Then an emitter may form in the crack which cannot be opened by the edge opening procedure. Moreover, metal paste may be squeezed through such a crack, leading to severe ohmic shunts. A third type of process-induced ohmic shunt is caused by Al-particles lying on the emitter surface. They may be e.g. residues of the base metallization. In the final firing step, such particles alloy into the surface where they may overcompensate the emitter and lead to a p^+-layer around the particle. This p^+-layer is in contact to the base and makes an ohmic tunnel junction to the emitter, thereby shunting the junction. Generally, any extended defect showing a high local density of states and crossing the p-n junction,

which shows hopping conductivity, may cause also an ohmic conductivity. Therefore the junction between non-linear (recombination-induced) and ohmic shunts may be floating; some recombination-induced shunts like the edge region may have also an ohmic contribution.

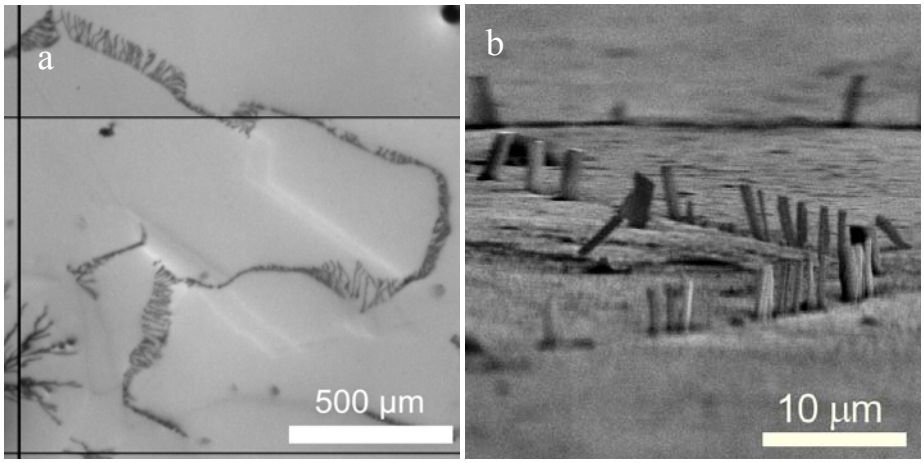

Fig. 6: (a) Infrared transmission light microscopy image of SiC filaments in a grain boundary, (b) SEM image of SiC filaments in a grain boundary after surface etching

The most important material-induced ohmic shunt type in MC material is caused by SiC filaments crossing the whole cell. These filaments may be several mm long with some µm in diameter and are growing during block crystallization preferentially in grain boundaries [25]. Due to the incorporation of N, which is the dominant shallow donor in SiC, these filaments are n^+-conducting and are in direct contact to the emitter [26]. Not all, but some of them also have ohmic contact to the base metallization of the cell, whereby the whole cell is shunted. It is not known yet under which conditions the filaments are in contact to the base metallization. These filaments can easily be detected by mirror polishing the material containing a shunt on both sides and imaging it in an ordinary light microscope in transmission mode with a CCD camera, see Fig. 6 (a). This works since the silicon wafer becomes transparent at a wavelength above 1000 nm where the CCD camera is still sensitive. For this purpose a back-and-white CCD camera has to be used whose IR-filter must be removed. After this investigation the silicon material may be partly removed by etching with HF-HNO_3. Then the filaments, which are not attacked by the etchant, stick out of the surface, see Fig. 6 (b). The n-type nature of the filaments may be proven by polishing away only the base contact and performing EBIC (Electron Beam-Induced Current) on the cell from the backside. Then the SiC filament show a bright EBIC signal [25]. Since C shows a small segregation coefficient in liquid Si, the probability to find SiC precipitates, which are also disturbing in the wire sawing process, is highest at the top of the ingot. A feasible way to avoid these precipitates is to reduce the amount of C contamination in the casting process.

Conclusions

In recent years the degree of understanding non-ideal I-V characteristics of industrial silicon solar cells has made significant progress. It has been found that all major aspects of non-ideal characteristics are due to extended crystal defect, which may be either material-induced or of technological origin. This holds for all three aspects of non-ideality, which are the unexpectedly large recombination current, often showing an unexpectedly large ideality factor, the reverse-bias breakdown behavior, and the presence of ohmic shunts.

In order to obtain the high current-densities and ideality factors above 2 at a forward bias below 0.6 V, recombination in heavily defected regions must be modeled beyond the SRH approximation of independent defect states. As a first approximation, we chose coupled donor- acceptor defect states that are both situated deep in the bandgap. Most realistic, non-specific, smooth distributions

of coupled recombination parameters yield the two commonly observed features of ideality factors: a peak in the range of 0.4 to 0.5 V, and a slow variation at lower forward biases.

While ohmic shunts are relatively well understood now, the quantitative understanding of large ideality factors has just begun, and only one of the different breakdown mechanisms in solar cells has been uniquely identified yet. There is still a demand for further research activities for a better understanding of the influence of defects on I-V characteristics of real solar cells.

This work was supported by the BMU project No. 037650 D "SolarFocus".

References

[1] W. Shockley, *The Theory of p-n Junctions and p-n Junction Transistors*, in: *Electrons and Holes in Semiconductors*. (D. Van Nostrand, Princeton, NJ, 1950)

[2] C.T. Sah, R.N. Noyce, W. Shockley, *Carrier Generation and Recombination in p-n Junction and p-n Junction Characteristics*, Proc. IRE. **45**, 1228 (1957)

[3] K. McIntosh: *Lumps, Humps and Bumps: Three Detrimental Effects in the Current-Voltage Curve of Silicon Solar Cells*, Ph.D. Thesis, UNSW, Sydney, 2001.

[4] C.T. Sah: *Fundamentals of Solid-State Electronics*. (World Scientific, Singapore 1992).

[5] M. Green: *Solar Cells - Operating Principles, Technology and System Applications*. (UNSW, Sydney, Australia 1998)

[6] R.A. Sinton, *Predicting multi-crystalline solar cell efficiency from lifetime measured during cell fabrication*, Proc. 3rd World Conf. on Photovolt. En. Conv., Osaka 2003, p. 1028.

[7] O. Breitenstein, J. Heydenreich, *Non-Ideal I-V-Characteristics of Block-Cast Silicon Solar Cells*, Solid State Phenomena **37-38**, 139 (1994).

[8] S.W. Glunz et al., *High-Efficiency Silicon Solar Cells for Low-Illumination Application*, Proc. 29th IEEE PPSC, New Orleans 2002, p. 450.

[9] O. Breitenstein, W. Eberhardt, K. Iwig, *Imaging the Local Forward Current Density of Solar Cells by Dynamical Precision Contact Thermography*, Proc. First World Conf. on Photovoltaic Energy Conversion (WCPEC), Hawaii 1994, p. 1633.

[10] O. Breitenstein, M. Langenkamp: *Lock-in Thermography - Basics and Use for Functional Diagnostics of Electronic Components*. (Springer, Berlin 2003).

[11] O. Breitenstein, J.P. Rakotoniaina, G. Hahn, M. Kaes, T. Pernau, S. Seren, W. Warta, J. Isenberg, *Lock-in Thermography - A Universal Tool for Local Analysis of Solar Cells*, Proc. 20th Eur. Photovoltaic Solar Energy Conference and Exhibition, Barcelona 2005, p. 590.

[12] O. Breitenstein, J.P. Rakotoniaina, *Electrothermal simulation of a defect in a solar cell*, J. Appl. Phys. **97,** 074905 (2005).

[13] O. Breitenstein, P. P. Altermatt, K. Ramspeck, A. Schenk, *The Origin of Ideality Factors > 2 of Shunts and Surfaces in the Dark I-V Curves of Si Solar Cells*, Proc. 21th Eur. Photovoltaic Solar Energy Conference and Exhibition, Dresden 2006, p. 625.

[14] H.J. Queisser, *Forward Characteristics and Efficiencies of Silicon Solar Cells*, Solid-State Electronics **5**, 1 (1962).

[15] A. Kaminski, J.J. Marchand, H. El Omari, A. Laugier, Q.N. Le, D. Sarti, *Conduction Processes in Silicon Solar Cells*, Proc. 25th IEEE PVSC, Washington DC 1996, p. 573.

[16] A. Schenk, U. Krumbein, *Coupled Defect -Level Recombination: Theory and Application to Anormalous Diode Characteristics*, J. Appl. Phys. **78**, 3185 (1995).

[17] R. Kühn, P. Fath, E. Bucher, *Effects of pn-Junction Bordering on Surfaces Investigated by Means of 2D-Modeling*, Proc. 28th IEEE PVSC, Anchorage 2000, p. 116.

[18] Sentaurus, TCAD, Synopsys Inc., Mountain View, CA, 2005.

[19] N.F. Mott: *Metal-Insulator Transitions*. (Taylor & Francis, London 1990).

[20] J. Bauer, J.-M. Wagner, A. Lotnyk, H. Blumtritt, B. Lim, J. Schmidt, O. Breitenstein, *Hot spots in multicrystalline silicon solar cells: avalanche breakdown due to etch pits*, Phys. Stat. Sol. RRL **3**, 40 (2009).

[21] D. Lausch, K. Petter, H. v. Wenckstern, M. Grundmann, *Correlation of pre-breakdown sites and bulk defects in multicrystalline silicon solar cells*, Phys. Stat. Sol. RRL **3**, 70 (2009).

[22] O. Breitenstein, J. Bauer, J.-M. Wagner, A. Lotnyk, *Imaging Physical Parameters of Pre-Breakdown Sites by Lock-in Thermography Techniques*, Prog. Photovolt: Res. Appl. **16**, 679 (2008).

[23] S.M. Sze, G. Gibbons, *Effect of Junction Curvature on Breakdown Voltage in Semiconductors*, Solid-State Electronics **9**, 831 (1966).

[24] O. Breitenstein, J.P. Rakotoniaina, M.H. Al Rifai, M. Werner, *Shunt Types in Crystalline Silicon Solar Cells*, Prog. Photovolt: Res. Appl. **12,** 529 (2004).

[25] Hejjo Al Rifai, O. Breitenstein, J.P. Rakotoniaina, M. Werner, *Investigation of Material-Induced Shunts in Block-Cast Multicrystalline Silicon Solar Cells Caused by SiC Precipitate Filaments*, Proc. 19th Eur. Photovoltaic Solar Energy Conference and Exhibition, Paris 2004, p. 632.

[26] J. Bauer, O. Breitenstein, J.P. Rakotoniaina, *Electronic activity of SiC precipitates in multicrystalline solar silicon*, phys. stat. sol. (a) **204**, 2190 (2007).